ISSN 1330–0008
CODEN FIZAE4

OVERLAPPED KAM PATTERNS FOR LINEARLY COUPLED ASYMMETRIC OSCILLATORS

VLADIMIR PAAR and NENAD PAVIN

Department of Physics, Faculty of Science, University of Zagreb, 10000 Zagreb, Croatia

Received 28 March 2000; revised manuscript received 19 June 2000
Accepted 19 June 2000

The pattern of energy dependence for the onset of chaos is investigated for conservative system of two linearly coupled asymmetric oscillators, harmonic oscillator and a two-well nonlinear oscillator. With increase of energy, the amount of chaoticity first grows up to a certain critical energy, according to the KAM scenario, and above this point, with a further increase of energy, the amount of chaoticity decreases according to the inverse KAM scenario. At the point of transition, there is an overlap of the two scenarios. The position of the critical energy increases with increasing value of the coupling strength between oscillators.

PACS numbers: 05.45.+b UDC 530.182, 531.143

Keywords: conservative systems, linearly coupled harmonic and nonlinear oscillators, KAM scenario, inverse KAM scenario

1. Introduction

A classical case of the regularity-to-chaos transition according to the Kolmogorov-Arnold-Moser (KAM) theorem [1] in conservative system is the Henon-Heiles model [2,3] which can be considered as two single-well oscillators coupled by a cubic interaction term in the Hamiltonian. Parameters in the Henon-Heiles model are kept fixed at constant values and, therefore, the extent of destruction of KAM tori depends only on energy. For low values of energy, most of the trajectories are associated with the KAM tori. The pattern of energy dependence seen with the Henon-Heiles model is as follows [2,3]. At low energy, the chaotic behaviour is barely noticeable because it is confined to very small regions of phase space. As the energy increase, the KAM tori begin to dissolve and the chaotic regions begin to expand. After the last KAM torus disappeared, a single chaotic trajectory covers the entire energetically allowed region of the phase space. Thus, for a sufficiently high energy, a fully chaotic pattern is achieved and a regularity-to-chaos transition is fully completed. This is referred to as the universal behaviour of energy dependence of chaoticity for nonintegrable Hamiltonian systems.

A qualitatively similar type of universal behaviour was obtained for chaotic pattern in the case of two single-well oscillators coupled by symmetric quartic interaction term in the Hamiltonian [4–6]. Similar phenomena have been investigated for the order-chaos-order sequence in the spring pendulum [7].

On the other hand, in the investigations of the double pendulum another pattern of chaotic behaviour was found [6] with a regularity-to-chaos-to-regularity transition. Furthermore, independence on the strength of interaction between coupled oscillators a chaos to regularity-to-chaos transition was also found [8].

In this paper we study the interplay between chaotic and regular behaviour with the increase of energy in the case of the coupling harmonic oscillator and nonlinear double-well oscillator by a linear interaction term. Each independent nonlinear oscillator is an autonomous system with one degree of freedom and, therefore, integrable. Therefore, the system of uncoupled nonlinear and linear oscillators is integrable, too. However, the introduction of coupling between oscillators can induce chaos in the system, the pattern of which depends on the coupling strength. The basic question is whether in this system the energy dependence of the onset of chaos exhibits a universal behaviour, similar as of the Henon-Heiles system, or it shows a more complex pattern. This point may be relevant also in a broader framework if a weak dissipation is added to the Hamiltonian system, leading to the appearance of truncated fractal basin boundaries [9,10]. Namely, if the dissipation is excluded, according to the KAM scenario, chaos can appear with increase of energy. Then the appearance of chaos is associated with the stretching and folding in the phase space. It is clear that the introduction of dissipation is associated with changes in the system, but it will not completely change its character. Because of the presence of dissipation in the system, periodic orbits cannot exist any more and, therefore, there is neither stationary chaos nor a homoclinic orbit. However, the truncated fractal basin boundaries remain as a kind of "shadows" of the Hamiltonian or transient chaos [11–22].

2. *Nonlinear system of linearly coupled harmonic and double-well nonlinear oscillators*

We study the evolution of chaoticity with increasing energy for a Hamiltonian system of a harmonic oscillator (y-oscillator) and a nonlinear double-well oscillator (x-oscillator) coupled by a linear interaction term, with the equations of motion

$$\begin{aligned} \ddot{x} - x + x^3 + \alpha(x-y) &= 0 \\ \ddot{y} + y + \alpha(y-x) &= 0 \end{aligned} \tag{1}$$

where α is the coupling strength. The linear term $\alpha(x-y)$ in the equations of motion corresponds to a quadratic term in the corresponding Hamiltonian. The linear coupling between the two oscillators in the equations of motion was previously considered for the nonlinear mass-spring system [23] and in connection with the scalar diffusion [24].

Equations of motion (1) describe the motion in the two-dimensional potential

$$V(x, y) = x^4/4 + [y^2 - x^2 + \alpha(x - y)^2]/2 . \tag{2}$$

This potential has two minima at the points $(x_{\min}, y_{\min})$ and $(-x_{\min}, -y_{\min})$ where $x_{\min} = 1/\sqrt{1+\alpha}$, $y_{\min} = \alpha/\sqrt{(1+\alpha)^3}$. The values of the potential energy at these points are equal to $V(x_{\min}, y_{\min}) = V(-x_{\min}, -y_{\min}) = -\frac{1}{4(1+\alpha)^2}$. The saddle point is at the position (0, 0) and the value of the potential energy at this point is $V(0, 0) = 0$. For small values of the coupling strength α, the positions of minima are approximately given by: $x_{\min} \approx 1 - \alpha/2$, $y_{\min} = \alpha$. With the increase of the coupling strength α, the positions of the minima are shifting, but even for very large values of α, they will differ from the saddle point.

For a fixed value of the coupling strength α and energy E, Poincaré sections $(x, \dot{x})$ are computed, defined by the intersection with the plane given by $y \cdot x_{\min} - x \cdot y_{\min} = 0$ with the condition $\dot{y} > 0$. The plane of Poincaré section defined in this way passes the points of minima of potential energy $(x_{\min}, y_{\min})$ and $(-x_{\min}, -y_{\min})$. To fill out the Poincaré section, a set of initial conditions extended over the energetically accessible region are chosen in each calculation.

For $\alpha = 0$, the two oscillators, denoted as x-oscillator (nonlinear double-well oscillator) and as y-oscillator (harmonic oscillator), are decoupled and the system (1) is integrable. For $\alpha > 0$, at a fixed value of energy, the fraction of chaotic regions in the Poincaré section gradually increases with the increasing coupling strength α.

The aim of the present investigation is to study how the fraction of chaotic regions evolves with increasing energy at a fixed value of the coupling strength. In Figs. 1, 2 and 3, we display some characteristic Poincaré sections with increasing energy at three fixed values of the coupling strength $\alpha = 0.05$ (weak coupling), $\alpha = 0.5$ (moderate coupling) and $\alpha = 5$ (strong coupling), respectively.

3. *Discussion*

Let us first discuss the computed results for the case of weak coupling $\alpha = 0.05$ (Fig. 1). At low energies, as in Fig. 1a, the Poincaré section exhibits an integrable pattern. The orbits are trapped in one of two potential wells of the x-oscillator, forming the corresponding families of elliptic orbits. Such orbits, restricted to one potential well, are referred to as small orbits. With the increase of energy, a secondary family of elliptic orbits appears around an additional elliptic point lying below the region of each central elliptic family (Fig. 1b). These families of elliptic orbits are referred to as the lower deformed families. Simultaneously, the KAM scenario starts to develop and patches of chaotic regime are noticeable, in particularly in the region around the saddle point between the two wells of potential energy and in the regions surrounding the regions of central and lower deformed families of orbits and between these families (Fig. 1b).

With a further increase of energy, the orbits moving through both potential wells of the x-oscillator become energetically accessible. Such orbits are referred

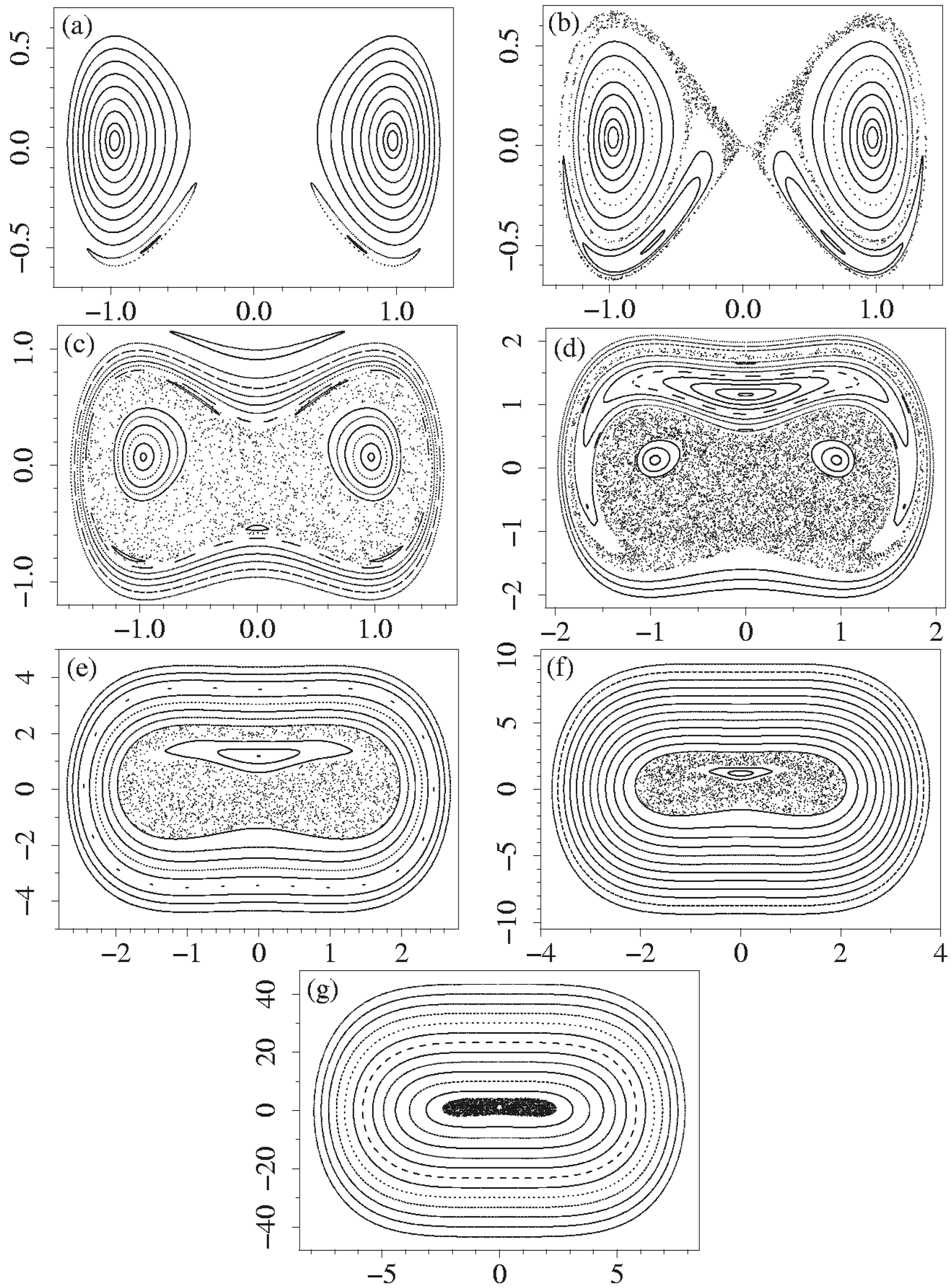

Fig. 1. Poincaré sections $(x, \dot{x})$ of the system (1) at $\alpha = 0.05$ (weak coupling) for increasing values of energy: a) $E = -0.05$, b) $E = 0$, c) $E = 0.5$, d) $E = 2$, e) $E = 10$, f) $E = 50$, g) $E = 1000$.

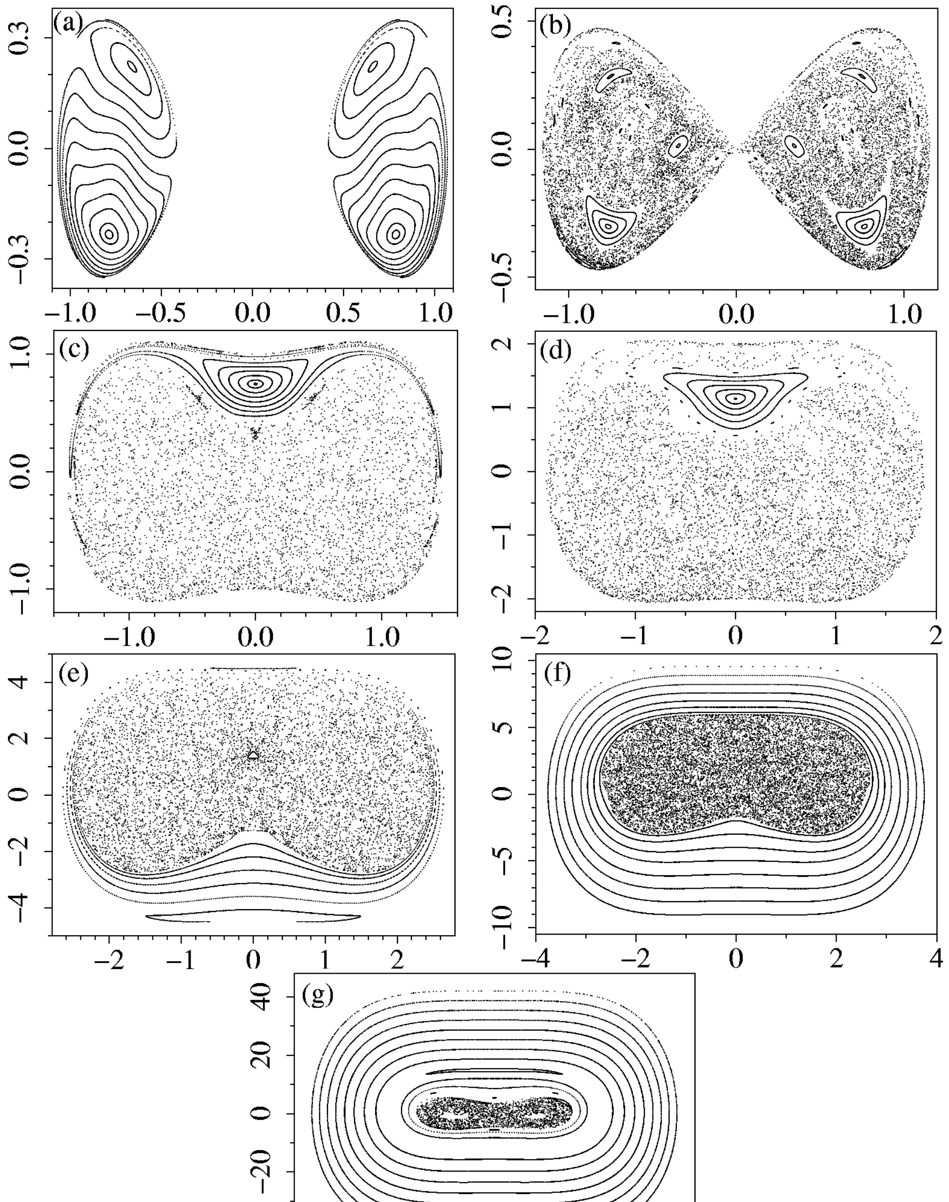

Fig. 2. Poincaré sections $(x, \dot{x})$ of the system (1) at $\alpha = 0.5$ (moderate coupling) for increasing values of energy as in Fig 1.

to as the large orbits. This is accompanied by a rapid onset of chaos, and the remaining KAM tori are restricted to two central islands of the x-oscillator, to smaller islands immersed into chaotic sea and to the region of large elliptic orbits encircling the chaotic sea (Fig. 1c).

When increasing the energy, the energetically accessible phase space region further increases, and according to the universal behaviour for energy dependence of degree of chaos for nonintegrable Hamiltonian systems, one would expect that the regions of regularity will gradually decrease in size, finally resulting in a fully chaotic pattern. Contrary to that, with a further increase of energy above a certain critical value, a new stretched island appears around the elliptic point placed above the saddle point of the x-oscillator (Fig. 1d). This regular island will be referred to as the upper deformed island.

As the energy increases further, the two islands formed by small orbits, referred to as central islands, gradually shrink, but contrary to the expectations according to the universal scenario, the newly borned upper deformed island survives. The chaotic sea occupies ever smaller percentage of the energetically accessible region of phase space, and more outer large elliptic orbits appear (Figs. 1e, f and g). Thus, in the case of weak coupling, with increasing energy, the onset of chaos follows the pattern of universal behaviour up to a certain energy, and above it the degree of chaos decreases with a further increase of energy.

In Fig. 2, Poincaré sections are presented for the case of the ten times stronger coupling than in Fig. 1, i.e., for $\alpha = 0.5$. The Poincaré section at low energy is still regular, as in the previous weak coupling case, but its pattern is different (Fig. 2a). Namely, the coupling between the oscillators acts in such a way that the family of small elliptic orbits around potential energy minimum of each well of the x-oscillator (with elliptic point at $\dot{x} = 0$) from the weak coupling case is replaced by two families of small deformed orbits, one with $\dot{x} > 0$ and the other with $\dot{x} < 0$ (Fig. 2a). With the increase of energy, chaotic regions are developed in accordance with the KAM theorem (Fig. 2b), but similarly as in the previous case, additional new upper deformed island appears around the elliptic point placed above the saddle point of the x-oscillator (Fig. 2c). However, with a further increase of energy above the critical value, the upper deformed island shrinks. Simultaneously, more and more outer large elliptic orbits are generated, taking an increased fraction of percentage of energetically accessible region of the phase space (Figs. 2e, f and g). However, the onset of the inverse KAM scenario takes place at higher critical energy than for the case of weak coupling shown in Fig. 1.

In the case of strong coupling, a qualitatively similar behaviour is seen, but the critical energy at which the KAM scenario switches into the inverse KAM scenario is at a much higher energy, above the energy $E = 50$ (Fig. 3).

Quite generally, as the energy increases to sufficiently high values, the structure of Poincaré sections is dominated by a family of large elliptic orbits. This pattern tends to the set of large elliptic orbits which correspond to the limit of decoupled integrable x-oscillator

$$\ddot{x} + x^3 = 0 \tag{3}$$

which arises from the system (1) in the large amplitude limit, corresponding to the limit of high energy.

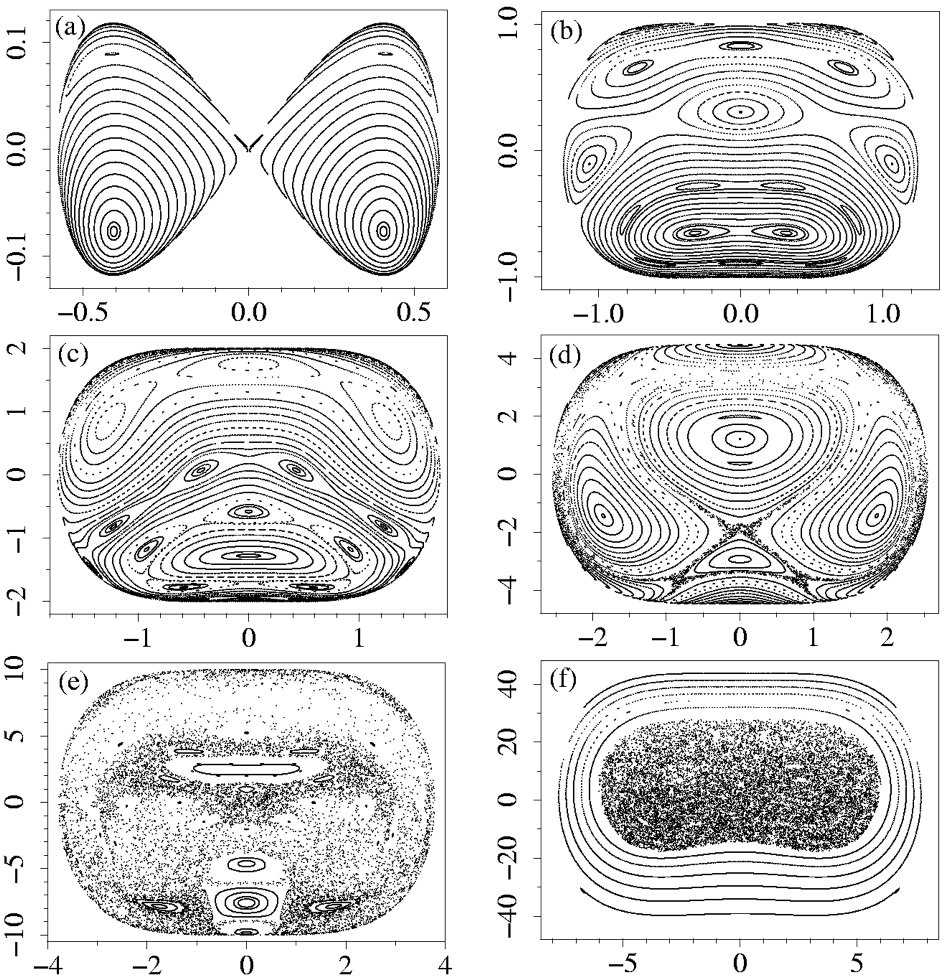

Fig. 3. Poincaré sections $(x,\, \dot{x})$ of the system (1) at $\alpha = 5$ (strong coupling) for the same increasing values of energy: a) $E = 0$, b) $E = 0.5$, c) $E = 2$, d) $E = 10$, e) $E = 50$, f) $E = 1000$. There is no Poincaré section for $E = -0.05$ because the local minimum of potential energy lies higher.

Thus, we can argue that the system (1) has two asymptotically integrable limits, the low-energy and the high-energy limit. With an increase of energy, the system evolves first in accordance with the KAM scenario, but before it is completed, an inverse KAM scenario sets in and dominates a further evolution of the system towards the high-energy integrable limit. A particular role in the overlap of KAM and inverse KAM scenario is played by an upper deformed island, which has the basic role in preventing the formation of fully developed chaos.

4. Conclusion

We investigate the pattern of energy dependence for the onset of chaos in a system of linearly coupled harmonic and double-well nonlinear oscillator. We have found that at low energies the pattern follows the KAM scenario of increase of chaoticity with increase of energy. However, at a certain critical value of energy, the KAM scenario switches into the inverse KAM scenario, with decrease of chaoticity when further increasing the energy. The value of the critical energy increases when increasing the coupling strength, and it is much higher in the case of strong coupling than in the case of weak coupling. These results may be of significance not only for the study of the Hamiltonian systems, but also for better understanding of the dissipative systems with weak dissipation, because some important phenomena, truncated fractal basin boundaries remain as a kind of "shadows" of the Hamiltonian chaos, while, on the other hand, there is a plethora of coupled oscillators in many systems in nature, like for example in biological systems [25–29].

References

[1] V. I. Arnold, *Mathematical Methods in Classical Mechanics*, Springer, Berlin (1978).

[2] R. C. Hilborn, *Chaos and Nonlinear Dynamics*, Oxford University Press, New York (1994).

[3] M. Henon, in: *Chaotic Behaviour of Deterministic Systems*, eds. G. Iooss, R. H. Helleman and R. Stora, North-Holland, Amsterdam (1983), pp. 53-170; M. Henon and C. Heiles, Astrophys. J. **69** (1964) 73.

[4] L. A. Bunimovich, Commun. Math. Phys. **65** (1979) 295.

[5] R. Z. Sagdeev, D. A. Usikov and G. M. Zaslavsky, *Nonlinear Physics*, Harwood Academic Publishers, Chur (1992).

[6] H. J. Korsch and H. J. Jodl, *Chaos*, Springer, Berlin (1994).

[7] J. P. van der Weele and E. de Kleine, Physica **A 228** (1996) 245.

[8] Z. Deng and F. T. Hioe, Phys. Rev. Lett. **55** (1985) 1539.

[9] I. Dobson and D. F. Delchamps J. Nonlinear Sci. **4** (1994) 315.

[10] M. Varghese and J. S. Thorp, Phys. Rev. Lett. **60** (1988) 665.

[11] C. Grebogi, E. Ott and J. A. Yorke, Phys. Rev. Lett. **50** (1983) 935.

[12] C. Grebogi, E. Ott and J. A. Yorke, J. A. Science **238** (1987) 632.

[13] C. Grebogi, E. Kostelich, E. Ott and J. A. Yorke, Physica **D 25** (1987) 347.

[14] E. Ott, J. Alexander, I. Kan, J. C. Sommerer and J. A. Yorke, Physica **D 76** (1994) 384.

[15] V. Paar, N. Pavin, N. Paar and B. Novaković, Robotica **14** (1996) 423.

[16] V. Paar, N. Pavin, N. Paar and B. Novaković, Robotica **17** (1999) 195.

[17] V. Paar and N. Pavin, Phys. Rev. **E 55** (1997) 4112.

[18] V. Paar and N. Pavin, Physica (Amsterdam) **A 242** (1997) 166.

[19] V. Paar and N. Pavin, Mod. Phys. Lett. **10** (1996) 153.

[20] V. Paar and N. Pavin, Phys. Lett. **A 235** (1997) 139.

[21] V. Paar and N. Pavin, Phys. Rev. **E 57** (1998) 1544.

[22] E. Ott, *Chaos in Dynamical Systems*, Cambridge University Press, Cambridge (1993).

[23] R. M. Rosenberg, Adv. Appl. Mech. **9** (1966) 155.

[24] R. Ermentrout, in: *Nonlinear Oscillations in Biology and Chemistry*, ed. H. G. Othmer, Springer, Berlin (1966) pp. 98-114.

[25] D. Avnir, O. Biham, D. Lidar, and O. Malcai, Science **279** (1997) 39.

[26] N. A. J. Gough, The Lancet **339** (1993) 182.

[27] A. L. Goldberger and B. West, Yale J. Biol. Med. **60** (1987) 421.

[28] M. Kaern and A. Hunding, J. Theor. Biol. **198** (1999) 269.

[29] D. J. Murray, *Mathematical Biology*, Springer, Berlin (1993).

PREKLAPAJUĆI KAM-SCENARIJI ZA LINEARNO VEZANE ASIMETRIČNE OSCILATORE

Struktura energijske ovisnosti evolucije kaosa istražuje se za konzervativni sustav dvaju linearno vezanih asimetričnih oscilatora, harmonijskog oscilatora i nelinearnog oscilatora s dvije jame. S porastom energije stupanj kaotičnosti najprije raste do određene kritične vrijednosti energije, sukladno KAM scenariju, a iznad te energije, s daljnjim porastom energije, udio kaotičnosti pada sukladno inverznom KAM scenariju. Pri prijelazu iz jednog scenarija u drugi dolazi do njihovog preklopa. Vrijednost kritične energije raste s porastom jakosti vezanja među oscilatorima.